Crystal Orientation Distribution and Elastic Anisotropy in Cu-Ni-Si Alloy Sheets

Hiroshi Kaneko[*1], *Tatsuhiko Eguchi*[*2], *Hirofumi Inoue*[*3]

ABSTRACT The authors researched the influence of crystal orientation distributions in precipitation-hardened Cu-Ni-Si alloy sheets for springs on their elastic anisotropy. The crystal orientation distributions were measured by the X-ray pole figure measurement and the Electron Backscatter Diffraction (EBSD) method, and the Young's moduli were measured by the resonance method and the tensile method at various composition ratios of several crystal orientations which developed during recrystallization. The Young's modulus was the lowest when the Cube orientation{001}<100> was developed and the highest when the R orientation{231}<346> was developed. The difference was 30 GPa and above, and showed a good correspondence to the Hill model based on the crystal orientation distribution function (ODF). Different from the existing method of controlling the Young's modulus by the increase of solution elements, this effect can broaden the variation of Young's modulus without losing a good electrical conductivity. Therefore, this effect greatly enhances the flexibility of the design of springs for electric contact sections and contributes to the advancement in operations of connectors.

1. INTRODUCTION

Recrystallization textures have been researched in many types of FCC metals, and several preferred orientations have been reported. These preferred orientations in copper alloys mainly correspond to alloy compositions. In pure copper alloys, it has been reported that the Cube orientation{001}<100> and the R orientation{231}<346> decrease, and, the BR orientation{362}<853> and the RD-rotated Cube orientation{012}<100> increase along with the increase in additive elements[1),3)]. On the other hand, the elasticities of copper alloys have strong crystal orientation dependence. The Young's moduli of single crystals vary from the lowest of 67 GPa for the <001> direction to the highest of 190 GPa for the <111> direction, which is three times larger[4)]. However, although it was important in practical use, few examples have been reported on the influence of polycrystal recrystallization textures consisting of fine crystals on the Young's moduli because, in general, they are difficult to vary in the same alloy composition[5),6)]. Confirming the influence of microstructural factors, such as the anisotoropy of grain shapes, in polycrystal recrystallization materials, is also an important subject.

This paper is the reprint of the paper published in the Journal of Japan Institute of Metals and Materials Vol. 77 No.9 (2013) issued by the Japan Inst. Met. Mater.

[*1] Laboratories for Fusion of Core Technologies, R&D Division.
[*2] Automotive Products & Electronics Laboratories, R&D Division.
[*3] Department of Materials Science, Graduate School of Engineering, Osaka Prefecture University.

Young's modulus is an important characteristic along with the yield strength for the copper alloys used in springs of electrical contacts. It varies depending on the types and the amount of additive elements[7)]. The application of Cu-Ni-Si alloys[8)] has been widely adopted because they have large amounts of precipitation hardening, and have a superior balance of the electric conductivities and the bending formabilities. In particular, high-density Cu-Ni-Si alloys containing Ni of about 4% have an advantage of being able to provide a high yield strength with fine and high-density precipitates of about 10 nm[9)], and Cu-3.8Ni-0.9Si alloys have a composition with the highest density among rod materials being mass-produced. However, the influence of high density on Young's modulus has not been clearly determined as well. Therefore, in this research, we made polycrystal sheets of Cu-Ni-Si alloys having different textures, and researched the influence of recrystallization textures on Young's moduli. With respect to Ni-Si density, we used a 3.8Ni base and a 2.3Ni base of medium density for comparison, and researched the influence of the volume fraction of the precipitates.

2. EXPERIMENTAL PROCEDURE

2.1 Sample Preparation

Table 1 shows the two levels of alloy compositions which were used in this study[10)] (hereinafter called the 2.3Ni alloy and the 3.8Ni alloy). First, rolled materials of 0.2 mm thickness were manufactured by repeating heat treatment and rolling for several times on the ingot casted in an

atmospheric furnace. Then, a solution treatment, which applies water quenching after keeping the materials in a salt bath, was performed at different temperatures depending on the composition. Finally, the materials were precipitation-hardened by aging treatment, by keeping them for two hours at 480℃, and provided as samples. The samples had recrystallization textures after the solution treatment, and no grain growth caused by the aging treatment was observed. As described later, the average grain size was 4-5 μm, which was considered fine. Samples in different recrystallization textures, L1-L4 (the 2.3Ni composition) and H1-H4 (the 3.8Ni composition), were manufactured by adjusting the conditions and the times of heat treatment and rolling in the process which led to the solution treatment stated above. No difference was observed among L1-L4 of the same composition with respect to the contribution of the solution elements and the dispersion state of the Ni-Si precipitates to the Young's moduli because the solubilities after the solution treatment were equivalent, and the conditions of the aging treatment were the same. The volume fractions of the Ni-Si precipitates, which were obtained by the variation in electrical conductivities before and after the aging treatment, were 0.027 in the 2.3Ni composition and 0.044 in the 3.8Ni composition. That is, the volume fraction of the 3.8Ni composition was about 1.6 times higher than that of the 2.3Ni composition. Also, the Vickers hardnesses (Hvs) after the aging treatment were about 220 in the 2.3Ni composition, and about 280 in the 3.8Ni composition, which was a high value.

Table 1 The Chemical Composition of the Samples (mass%)

	Ni	Si	Zn	Sn	Cr	Mg	Cu
2.3Ni alloy (UNS 64775)	2.30	0.65	0.50	0.15	0.15	0.10	Bal.
3.8Ni alloy (UNS 64790)	3.76	0.89	0.51	0.15	0.20	0.09	Bal.

2.2 Measurement of the Textures and the Grain Shapes

The samples were measured from the ND (normal direction) by the EBSD method after being mechanically polished and electro polished. The EBSD method provides a crystal orientation distribution information with the Kikuchi patterns on the fluorescent screen. These diffraction patterns are obtained by irradiating an electron beam in a scanning electron microscopy[11]. The measurement area was 800 μm × 800 μm, and the scan step was 1 μm. The total measurement points were 740,000, and the number of grains was 16,000 and over. The grain boundary was defined as a boundary which had a misorientation of 5°and over including twin boundaries. Grains of two pixels and over were targeted as the subject of the analysis. The axial densities of the grains and the area fractions of the main texture components in the RD (rolling direction) and the TD (transversal direction), in which the Young's moduli were evaluated as well, were analyzed (Tolerance Angle was 10°). OIM Analysis 5.3 of TSL, Inc. was used for the analyses above and for the ODF analyses stated below.

2.3 Measurement of the Young's Modulus

The resonance method is known for its high accuracy. This study used the measurement system shown in Figure 1. The sample was kept with a thin line at the point of node where it did not oscillate. Then, the eigenfrequency in free resonance was measured. JE-RT of Nihon Techno-Plus Co., Ltd. was used as the measurement equipment. The Young's modulus was obtained from Equation (1).

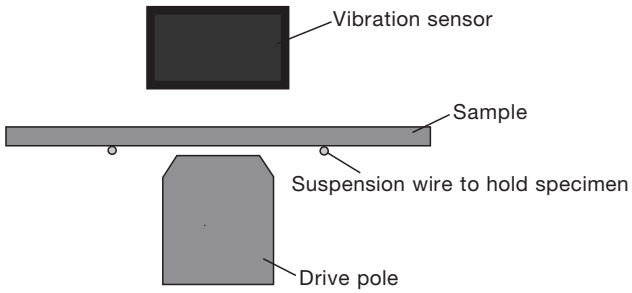

Figure 1 The Measurement system of a Young's modulus by the resonance method.

$$E = \left(\frac{48\pi^2 l^4 \rho}{t^2 n^4} \right) f_i^2 \quad (1)$$

In this equation, E : Young's modulus. l : sample length (22 mm), ρ: sample density (8.8 g/cm^3), t : board thickness (0.2 mm), n : solution to the equation (1) (4.73 in the first mode of vibration), f : eigenfrequency. The tensile test is also a common test method for the measurement of the Young's modulus. Therefore, the test results of the two measurement methods were first compared for reference. As Figure 2 shows, the results from the resonance method were about 2-12 GPa higher than those from the tensile test.

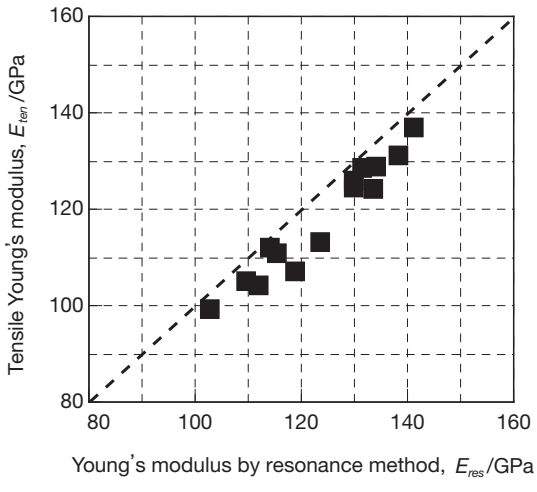

Figure 2 The comparison of the results of the tensile test and the resonance test in the measurement of the Young's moduli.

2.4 Calculation of the Elastic Compliance using the Orientation Distribution

$\overline{\sigma}_{ij}$, which is obtained by dividing the stress tensor by the whole sample, and $\overline{\varepsilon}_{ij}$, which is obtained by dividing the strain tensor by the whole sample in each micro region of the polycrystal sample, are supposed to satisfy the Hooke's law. The following two hypothetical models are known for the distribution of the stress and the strain in polycrystal materials. The Reuss model[12]: the stress works for each micro region equals to the stress works for the whole sample. The distribution of elastic strain is formed in the grain. The Voigt model[13]: The strain in each micro region is equal to the macroscopic strain in the whole sample. Distribution of stress is formed in the grain. Letting the compliance be s^R_{ijkl} and the stiffness be c^V_{ijkl} in the rank-4 tensor in both models, the Hooke's formula is formulated as:

$$\overline{\varepsilon}_{ij} = s^R_{ijkl}\overline{\sigma}_{kl} \tag{2}$$

$$\overline{\sigma}_{ij} = c^V_{ijkl}\overline{\varepsilon}_{kl} \tag{3}$$

Figure 3 (a) shows the configuration of the grains in both models. In an actual polycrystal material, we assumed a grain in a uni-axial shape as in Figure 3 (b). In this research, we applied the Hill model[14], in which the averaged stress and strain distributions in the Reuss and the Voigt model are assumed to give a good approximation. Its compliance is obtained by:

$$s^H_{ijkl} = \frac{1}{2}[s^R_{ijkl} + (c^V_{ijkl})^{-1}] \tag{4}$$

There are two kinds of methods to obtain s^R_{ijkl} and c^V_{ijkl}, depending on the measuring method of a crystal orientation distribution. When a crystal orientation distribution is measured by the EBSD method, the compliance is obtained by averaging the compliance $s^m_{ijkl}(g)$ at the mth measurement point, which is the crystal orientation g, over the whole measurement points: $\boldsymbol{n}$ (c^V_{ijkl} as well).

$$s^R_{ijkl} = \frac{1}{n}\sum_{m=1}^{n} s^m_{ijkl} \tag{5}$$

s^m_{ijkl} is obtained by the direction cosine $a_{i_n j_n}(g)$ between the axis of the sample coordinate system and the axis of crystal coordinate system which are obtained by the Euelr angle at each point.

$$s^m_{i_1 i_2 i_3 i_4} = a_{i_1 j_1}\cdot a_{i_2 j_2}\cdot a_{i_3 j_3}\cdot a_{i_4 j_4}\cdot s^0_{j_1 j_2 j_3 j_4} \quad (i_1 \sim i_4,\ j_1 \sim j_4 = 1,2,3) \tag{6}$$

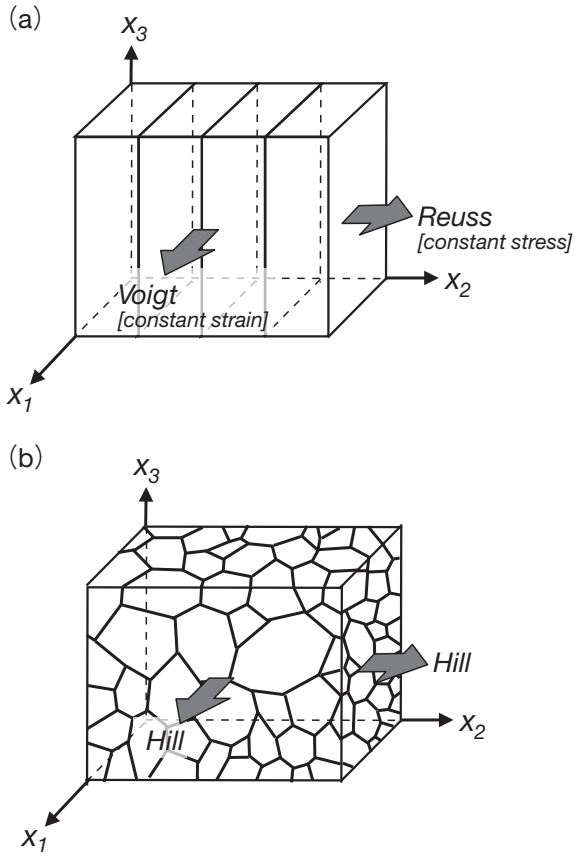

Figure 3 The Grain configuration. (a) Reuss and Voigt model, (b) Hill model.

Here, s^0 is the compliance in the axis of the crystal coordinate system (The description of Equation (6) is based on the Einstein summation convention). However, in the case of evaluating not only recrystallization textures as in this study but deformed textures and textures consisting of fine crystals generated by electro deposition, etc., it is common to use the orientation distribution function (ODF), which is based on an X-ray pole figure[15]. Therefore, in this study, we applied the methods indicated by Bunge[5), 16)], and obtained s^R_{ijkl} and c^V_{ijkl} using the coefficients of the ODF. The following shows the outline.

Equation (7) describes the ODF $\boldsymbol{f}(g)$ in the series of generalized harmonic functions $T^{mn}_l(g)$ using coefficients $A^{m\mu}_l$ and $A^{n\nu}_l$, regarding the symmetry between a crystal and a sample.

$$f(g) = \sum_{l=0}^{L}\sum_{\mu=1}^{M(l)}\sum_{\nu=1}^{N(l)}\sum_{m=-l}^{+l}\sum_{n=-l}^{+l} C^{\mu\nu}_l A^{m\mu}_l A^{n\nu}_l T^{mn}_l(g) \tag{7}$$

On the other hand, the product of the direction cosine in Equation (6) is described as:

$$a_{i_1 j_1}\cdot a_{i_2 j_2}\cdots a_{i_r j_r} = \sum_{l=0}^{r}\sum_{m=-l}^{+l}\sum_{n=-l}^{+l} a^{mn}_l(i_1 i_2\cdots i_r; j_1 j_2\cdots j_r) T^{mn}_l(g) \tag{8}$$

And, r=4 because the compliance is a rank-4 tensor. Also, when the compliance in a crystal coordinate system is resolved in an isotropy and an anisotropy part using the index of anisotropy S_a, they are described as in Equation (9) and (10).

$$s^0_{ijkl} = s^I_{ijkl} + s_a t_{ijkl} \quad (9)$$

$$s_a = s^0_{1111} - s^0_{1122} - 2s^0_{1212} \quad (10)$$

Because s^I_{ijkl} is independent from the crystal orientations, the average value of the whole sample s^R_{ijkl} is obtained by Equation (11) and (12) (c^V_{ijkl} as well).

$$s^R_{ijkl} = \bar{s}_{ijkl} = s^I_{ijkl} + s_a \bar{t}_{ijkl} = s^0_{ijkl} + s_a(\bar{t}_{ijkl} - t_{ijkl}) \quad (11)$$

$$\bar{t}_{ijkl} = \bar{a}(ijkl) = \sum_{l'=0}^{4} \sum_{\mu=1}^{M(l)} \sum_{\nu=1}^{N(l)} \bar{a}^{\mu\nu}_{l'}(ijkl)\, C^{\mu\nu}_{l'} \quad (12)$$

$\bar{a}^{\mu\nu}_{l'}(ijkl)$ is a purely mathematical quantity which is independent from the elastic constant and the crystal orientation distribution of the single crystals, and is described in a document[16]. Because the influence of the solution atoms, which are dissolved after aging, on a Young's modulus is estimated to be small[7], the value for pure copper indicated in Table 2 was applied for the elastic constant s^0 of a single crystal. The nine components of the elastic compliance s^H_{ijkl} were obtained from these analyses and compared the Young's moduli $1/s_{1111}$ and $1/s_{2222}$ in the RD and the TD to the Young's moduli of the experimental results. At calculation, the difference between the Voigt model value and the Reuss model value was 30 – 35 GPa. In this study, we confirmed previously that the approximation error caused by the series expansion was very small: The deviation between the results of Equation (5), which averages discrete crystal orientation distributions directly, and Equation (11)-(12), which makes a crystal orientation distribution into a continuous function in a series expansion, was 1% and less. In the case of a random orientation, the calculation result was $E_{Hill\text{-}Random}$= 127.0 GPa from the following Equation (13) and (14).

$$E_{Reuss-Random} = \frac{5}{3s^0_{1111} + 2s^0_{1122} + 4s^0_{1212}} \quad (13)$$

$$E_{Voigt-Random} = \frac{(c^0_{1111} - c^0_{1122} + 3c^0_{1212})(c^0_{1111} + 2c^0_{1122})}{2c^0_{1111} + 3c^0_{1122} + c^0_{1212}} \quad (14)$$

Table 2 The Elastic compliance and the stiffness in a crystal coordinate system used to calculate the Young's modulus.

s^0_{1111}	s^0_{1122}	s^0_{1212}	c^0_{1111}	c^0_{1122}	c^0_{1212}
0.015	−0.0063	0.0033	168.4	121.4	75.4

s [GPa^{-1}] c [GPa]

3. EXPERIMENTAL RESULT AND DISCUSSION

Figure 4 and 5 shows the measurement results of the crystal orientation distribution. The developments of the Cube orientation{001}<100>, the RD- rotated Cube orientation{012}<100>, the BR orientation{362}<853>, the R orientation{321}<346> and the Cu orientation{121}<111> were confirmed. Table 3 shows the area fractions in which these crystal orientation components are standardized by the whole measurement area. Even when the alloy compositions were same, major orientations and the degrees of development were greatly different in L1-L4 and H1-H4. That is, a strong Cube orientation in L1 and H1, a Cube orientation and an R orientation in L2 and H2, a weak and comparatively random R-Cu orientation in L3 and H3, and a strong BR-R orientation in L4 and H4, were confirmed.

Table 4 shows the calculation results of the elastic compliances by the Hill model after analyzing the textures with the ODF. Figure 6 and 7 show the measurement from the resonance method and the calculation results of the Young's moduli. It was confirmed that the Young's moduli in the 2.3Ni composition and the 3.8 composition evaluated by the resonance method were greatly different depending on the sample. The difference was 30 GPa and more in the absolute value and about 30% in ratio. The Young's moduli were low in L1 and H1 in which <001>//RD·TD were developed by the Cube orientation, moderate in the RD of L3 which had a comparatively random orientation, and high in the RD of H3, L4 and H4 which had few Cube orientations and comparatively abundant Cu orientations of RD<111> and R orientations in which the RD is close to <111>. Such tendencies were equivalent to those of single crystals. These variations in Young's moduli were favorably corresponding to the calculation results of the Hill model. The deviation was 5 GPa and less under the condition of eliminating H3-TD, and the ranking among the samples was corresponding. These results indicate that a large variation in a Young's moduli was closely corresponding to recrystallization textures. They were confirmed to vary from the high sides to the low sides compared to the analytic values of the random orientation. The correspondence of the measured values to the values of the Hill model indicates that the elastic deformation in this alloy system proceeded in the state where the stress distribution and the strain distribution coexisted. In addition, although the measurement of the Poisson's ratios in sheets is difficult, it is assumed that they did not vary widely as in the Young's moduli because the estimated Poisson's ratios in each direction by $-s^H_{1122}/s^H_{1111}$ and etc. from the results of Table 4 were in the range of 0.33 to 0.39.

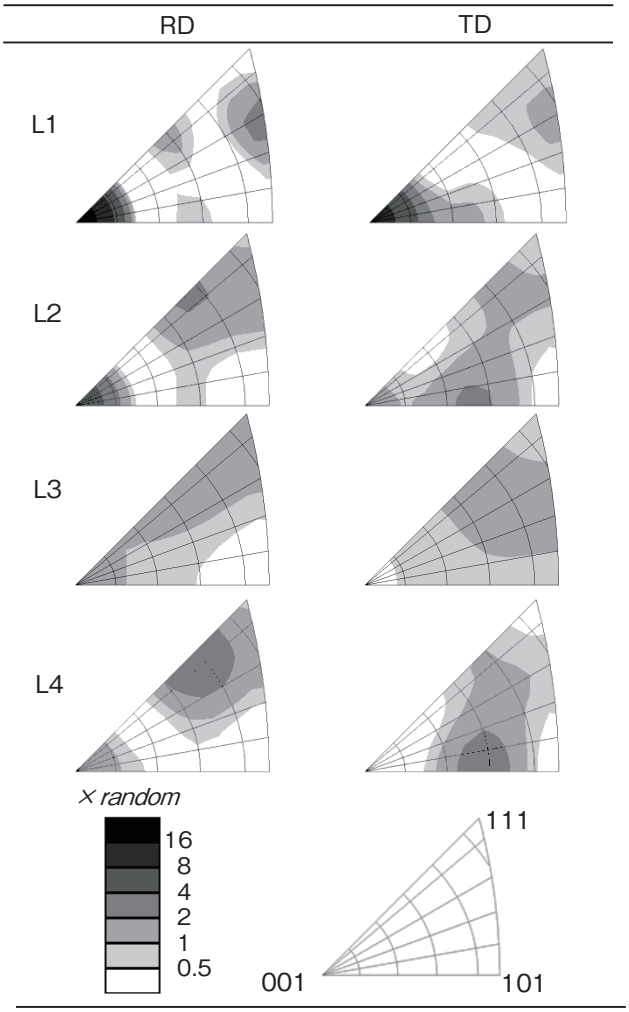

Figure 4 **The Contour plots of the crystal axial densities of 2.3Ni alloys in the RD and the TD from the inverse pole figures.**

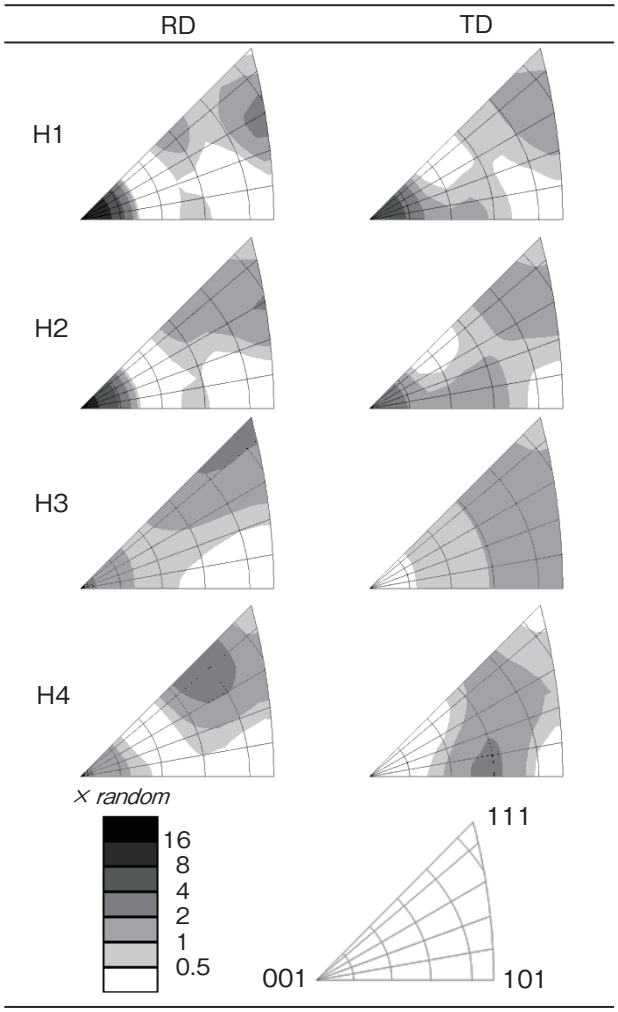

Figure 5 **The Contour plots of the crystal axial densities of 3.8Ni alloys in the RD and the TD from the inverse pole figures.**

Table 3 **The Area fractions (%) of each crystal orientation component. (The threshold angle is 10°).**

	Cube	RD-Cube	BR	R	Cu
L1	36	3	4	10	0
L2	20	6	7	11	0
L3	1	2	4	13	3
L4	0	5	33	15	1
H1	25	7	7	10	1
H2	12	10	14	12	0
H3	1	3	6	13	3
H4	1	5	32	19	0

We discuss the reasons of the measurement values being generally high compared to the analytical results of the Hill model, and the reasons of the slightly different deviations (called $\Delta E_{Hill\text{-}Random}$) depending on the sample and the direction. The first discussion is about the grain shape which was different from the isometric shape assumed in the Hill model. Figure 8 and 9 show the maps of the grain boundaries which have misorientations of 5°and more in the EBSD measurement (only a part of the whole measured area is shown). As Figure 10 shows, the grain includes a plate anneal twin inside an isometric crystal, and is not locally isometric. Figure 11 shows the average grain sizes in the RD and the TD from the cut method for reference. In L1 and H1 which have developed Cube orientations, the measurement values of the RD and the TD were equivalent (It was more remarkable in L1). On the other hand, in other samples, in general, the radii of the RDs tended to be larger than those of the TDs. That is, the RDs tended to have the arrangements close to those of the Reuss model, and the TDs had the arrangements close to those of the Voigt model. To analyze the directions of the plate twins which caused shape anisotropies in a three-dimensional way, we assumed the <111> in the crystal coordinate system was a minor axis direction of a plate twin, and showed the directions in the sample coordinate system in pole figures in Figure 12. For example, as Figure (e) shows, the angles of plate twins inside a Cube orientation grain toward the TD are 90°in 50% of the cases, which has the distribution of the Voigt model, and 35° in the other 50% of the cases. Each recrystallization orientation component had one to four variants (crystallographically equivalent crystal orienta-

tions), and each variant had twins in four directions. Figure 12 shows the average angles of these 16 twins. Although there are slight differences in the average angles depending on the orientation components of the recrystallization textures, the average angles are about 58°in all the orientation components. That is, the shape anisotropies of anneal twins were closer the side of the Voigt model (closer to the side of the high Young's modulus than the Hill model) in all the orientation components. Therefore, what needed to be researched to confirm the effects of the shape anisotropy was whether $\Delta E_{Hill\text{-}Random}$ became higher along with the increase in anneal twins. We obtained the lengths of the grain boundaries and researched their relationships with $\Delta E_{Hill\text{-}Random}$ in both compositions. As a result, no positive relationship was confirmed. Therefore, we conclude the effects of the shape anisotropy by anneal twins are small.

Next discussion is about the interference of deformation between the grains which is not considered in the Hill approximation. The degree of the effect may vary depending on the combination of orientations or the orientations of the boundaries of neighboring grains. In particular, analyses by the Mori-Tanaka concept and the applications of the Eshelby's equivalent inclusion idea have pointed out that the measured Young's modulus becomes higher than the Young's modulus estimated by the average orientation because the deformation in the stress direction is restrained when the grains in different Poisson's ratios neighbor in the grain boundary which is vertical to the stress direction (the Reuss distribution) [17]. Obtaining the Poisson's ratio of each crystal orientation by the tensor calculation in Equation (6), it was 0.82 when <the stress direction> was <011> and [the vertical direction] was [100], and -0.13 when <the stress direction> was <011> and [the vertical direction] was [0-11], which means the anisotropy was significant. When the stress axes were <001> and <111>, anisotropy was not present. The distribution of this effect may be comparatively large in H3-TD which had the maximum $\Delta E_{Hill\text{-}Random}$ because its neighboring frequency had distinctive characteristics due to the smallest area ratio of <011> in all the samples and also to its small grain size. The verification of this influence needs comprehensive researches for the amount of <011> development in the stress direction, the disposition of the grains, the grain size, and etc., and this will be an issue for future works. However, in this study, the influence is assumed to be small because the main orientations in the stress direction are <001> and <111> as Figure 4 and 5 show, which means the <011> is not a main orientation.

Table 4 The Components of the elastic compliances calculated by the Hill model.

Sample	s^H_{1111}	s^H_{2222}	s^H_{3333}	s^H_{1122}	s^H_{1133}	s^H_{2233}	s^H_{1212}	s^H_{1313}	s^H_{2323}
L1	0.0097	0.0094	0.0097	−0.0035	−0.0038	−0.0035	0.0048	0.0046	0.0048
L2	0.0089	0.0086	0.0089	−0.0031	−0.0034	−0.0031	0.0052	0.0049	0.0052
L3	0.0078	0.0076	0.0078	−0.0026	−0.0028	−0.0026	0.0056	0.0054	0.0056
L4	0.0074	0.0078	0.0078	−0.0025	−0.0025	−0.0029	0.0057	0.0058	0.0053
H1	0.0094	0.0089	0.0093	−0.0033	−0.0036	−0.0032	0.0049	0.0047	0.0050
H2	0.0087	0.0083	0.0086	−0.0030	−0.0033	−0.0029	0.0052	0.0050	0.0053
H3	0.0078	0.0075	0.0078	−0.0026	−0.0028	−0.0025	0.0057	0.0054	0.0057
H4	0.0075	0.0077	0.0077	−0.0025	−0.0025	−0.0027	0.0057	0.0057	0.0055

[GPa^{-1}]

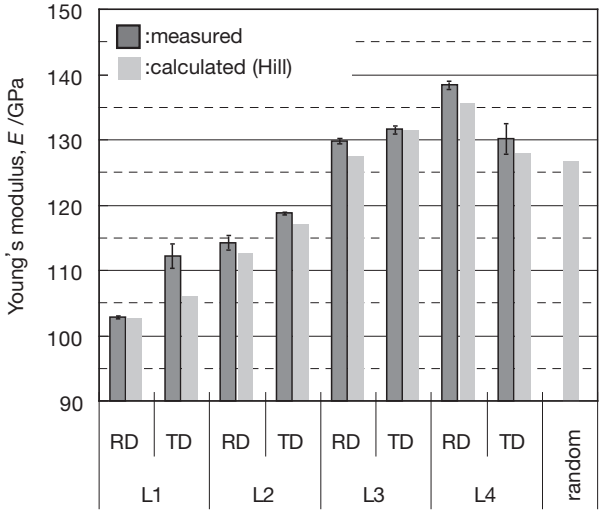

Figure 6 The measured and calculated Young's moduli of the 2.3Ni alloys.

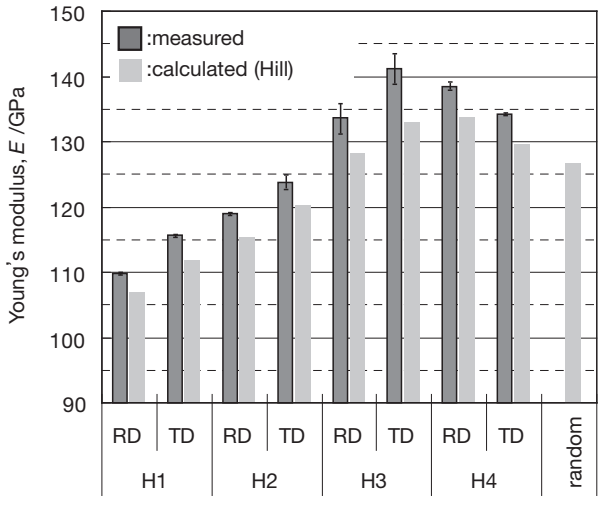

Figure 7 The measured and calculated Young's moduli of the 3.8Ni alloys.

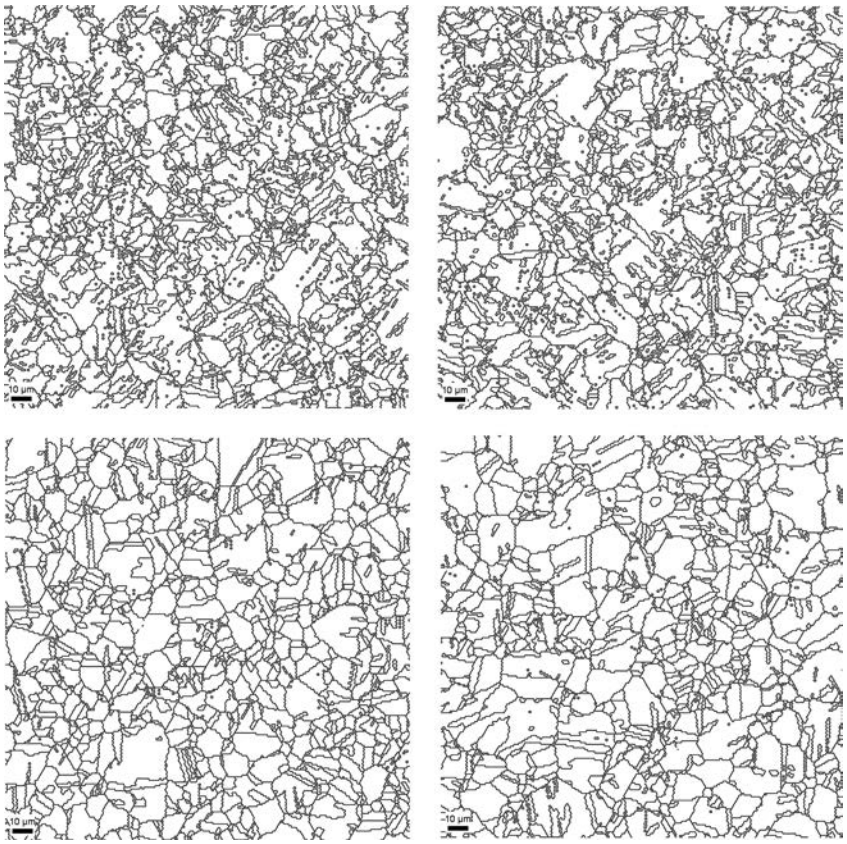

Figure 8 The grain boundary maps obtained by the EBSD measurements of the 2.3Ni-alloys, (a) L1, (b) L2, (c) L3, and (d) L4.

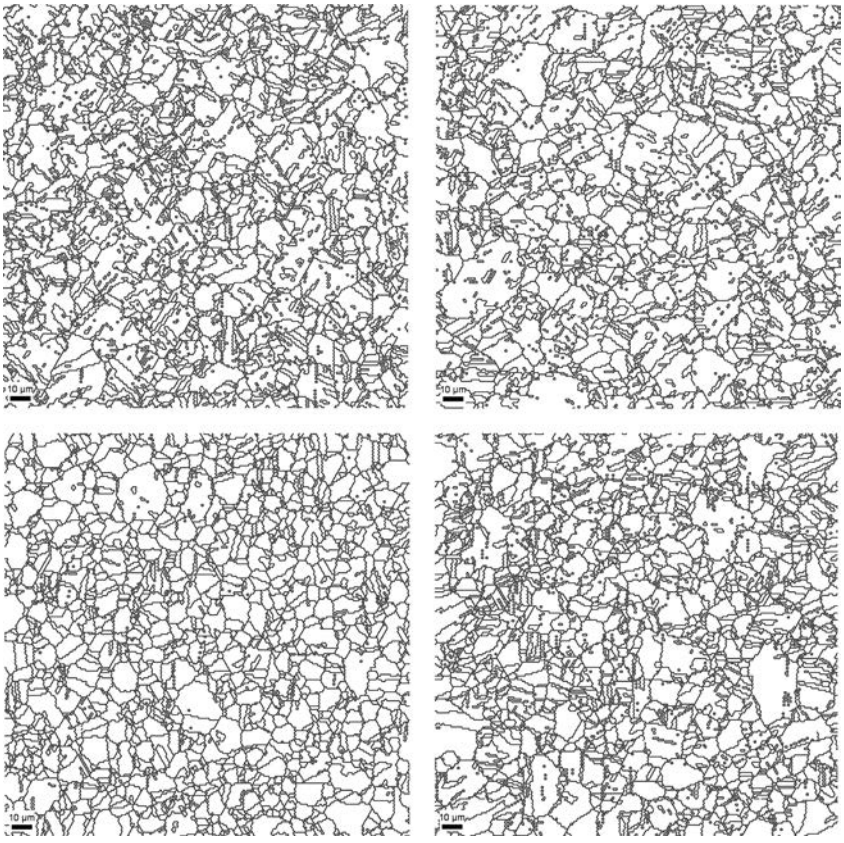

Figure 9 The grain boundary maps obtained by the EBSD measurements of the 3.8Ni-alloys, (a) H1, (b) H2, (c) H3, and (d) H4.

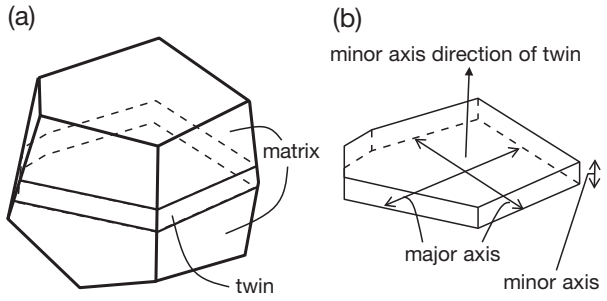

Figure 10 (a) An example of a matrix and its twin crystal, (b) The directions in a twin crystal plate.

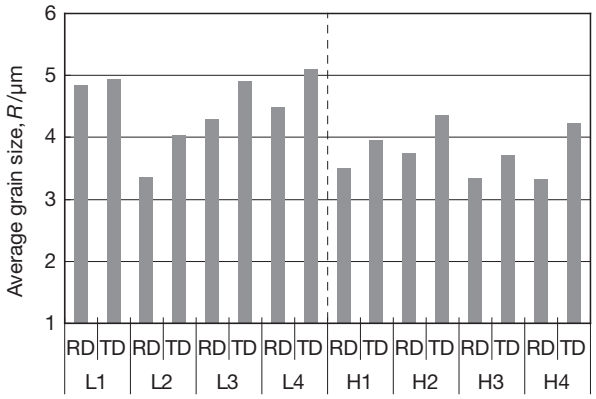

Figure 11 The average grain sizes measured by the intercept method along the RD and the TD.

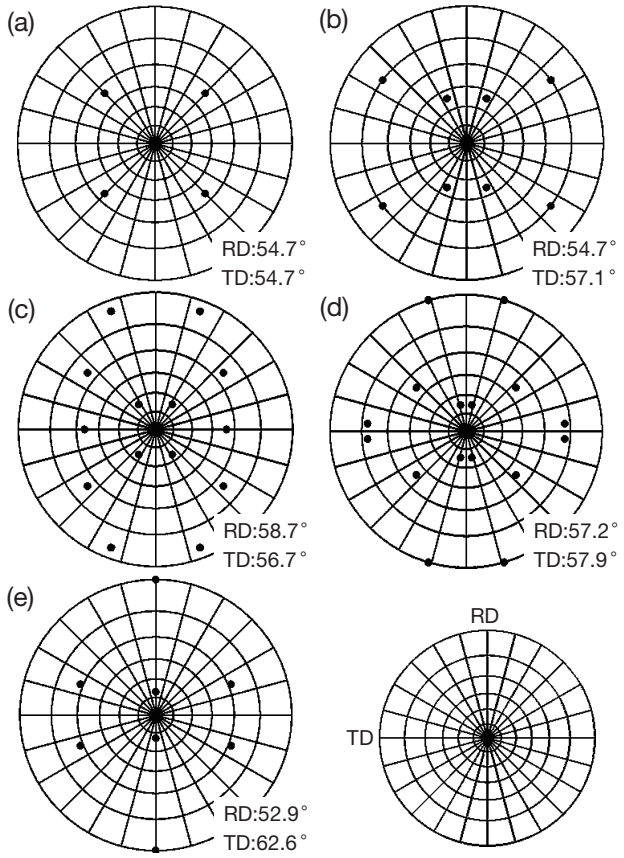

Figure 12 The pole figures (PFs) of twin plane normal in each grain (a): Cube, (b): RD-rotated Cube, (c): BR, (d): R (e): Cu orientation. The average angles between the stress direction (RD or TD) and the minor axis directions are shown in the lower right of each PF.

Finally, the relativities of the alloy compositions were compared. The average of $\Delta E_{Hill\text{-}Random}$ in the 2.3Ni composition was 2 GPa and that of the 3.8Ni composition was 4 GPa (the average excluding H3-TD). That is, $\Delta E_{Hill\text{-}Random}$ tended to increase with the increase in density. From the discussion above, the influence of the volume fraction of the precipitated phase is supposed to be large because the differences depending on the composition were not apparent in the grain shape anisotropy and in the interference between grains. Given the Young's modulus of the Ni2Si phase, which is a main precipitated phase, is 161 GPa[18], it is reasonable from a qualitative perspective that the Young's modulus increases along with the increase in the volume fraction. However, according to the common rule of mixture of the Young's modulus using a volume fraction, the increase in the Young's modulus is estimated to be about 1 GPa even in the 3.8Ni composition. Therefore, further research is needed for the densely and finely dispersed state to the increase in the Young's modulus.

We confirmed that textures have the largest influence on the Young's modulus control among various microstructural factors in the recrystallization materials of high-strength precipitated copper alloys. The reduction in Young's modulus is effective for downsizing and enhancing the operation of connectors[19]. The improvement effect for the bending workability by controlling textures is large as well[20]. Therefore, we expect that these copper alloys with controlled textures[19, 21], will contribute to the technical innovation of various electrical contacts and connectors.

4. CONCLUSION

We researched the influence of recrystalization textures and Ni-Si densities on Young's moduli using polycrystalline sheets of Cu-Ni-Si alloys with different textures in which the Cube orientation{001}<100>, the RD-rotated Cube orientation{012}<100>, the BR orientation{362}<853>, the R orientation{231}<346>, the Copper orientation{121}<111>, respectively, have been developed. The following are the main results.

(1) The Young's modulus is the lowest when a Cube orientation is developed and the highest when R-Copper orientations is developed. The Young's modulus varies by 30 GPa and over by controlling recrystallization textures.

(2) When a Young's modulus is calculated by the Hill model using the coefficient of the ODF based on the data of a crystal orientation distribution obtained by the EBSD method, it shows a good correspondence to the measured value.

(3) The measured Young's modulus and the Young's modulus calculated by the Hill model have a similar tendency in the 2.3Ni composition and the 3.8Ni composition. The influence of the increase in a volume fraction in a precipitation reinforced phase on a Young's modulus is considerably small compared to the influence textures.

REFERENCE

1) H. Eichelkraut, J. Hirsch and K. Lücke: Z. Metallkd. **75** (1984) 113–123.
2) O. Engler: Acta mater. **49** (2001) 1237-1247.
3) K. H. Virnich and K. Lücke: Proc. the Sixth International Conference on Textures of Materials (ICOTOM-6), (1981) p. 560
4) G. Simmons and H. Wang: Single Crystal Elastic constants and Calculated Aggregate Properties, (MIT Press, Cambridge, 1971).
5) H. Inoue, J. Iwata: J. Japan Inst. Copper **50** (2011) 204-209.
6) H. Kaneko, T. Eguchi: J. Japan Inst. Copper **51** (2012) 20-24.
7) L. M. T. Hopkin, H. Pursey and M. F. Markham: Z. Metallkd. **61** (1970) 535–540.
8) M. G. Corson: Inst. Metals Div., AIME, (1927), p435
9) H. Fujiwara, T. Sato and A Kamio: J. Japan Inst. Metals **62** (1998) 301-309.
10) H. Kaneko, K. Hirose, N. Tanaka and T. Eguchi: Proc. 58th IWCS/IICIT (2008) pp. 351-357.
11) V. Randle: Microstructure Determination and Its Application, (The Institute of Materials, London, 1992).
12) A. Reuss: Z. Angew. Math. Mech. **9** (1929) 49-58.
13) W. Voigt: Lehrbuch der Kristallphysik, (B. G. Teubner, Leipzig, 1910).
14) R. Hill: Proc. Phys. Soc., **A65** (1952), pp. 349-354.
15) H. Inoue: J. Japan Inst. Light Metal **60** (2010) 666-675.
16) H. J. Bunge: Texture Analysis in Materials Science, (Butterworths, London, 1982) pp. 294-329.
17) S. Onaka, K. Ando: J. Japan Inst. Metals **63** (1999) 1283-1289.
18) L. J. Chen: Silicide Technology for Integrated Circuits, (Peter Peregrinus Ltd, 2005) pp. 102
19) Furukawa Review No. 39 March (2011) p12-13 "The Copper Alloy Strip EFCUBE-820 for Connectors"
20) H. Kaneko, T. Eguchi: Mater. Trans. **53** (2012) 1847-1851.
21) Furukawa Review No. 42 September (2012) p18-19 "Development of a High Performance Copper Alloy EFCUBE-ST for Connectors"